

Co-design for Security and Performance: Geometric Tools [★]

Navid Hashemi ^a, Justin Ruths ^b,

^a*The University of Texas at Dallas, Department of Mechanical Engineering*

^b*The University of Texas at Dallas, Departments of Mechanical and Systems Engineering*

Abstract

When control systems are endowed with model-based anomaly detectors, the scale of what an attacker is able to accomplish is constrained if an attack is to remain stealthy to the detector. This paper develops a novel framework based on geometric sums for computing precise ellipsoidal bounds on the set of states reachable due to constrained stealthy attacks. We show that this approach provides much more exact ellipsoidal bounds than alternative methods based on convex optimization. The increased tightness of these bounds enables a thorough investigation into the inherent trade-off between closed-loop performance (measured based on the $\|H\|_2$ gain) and security (measured based on the reachable set of the attack) through the design of the controller and observer gain matrices in estimate-based feedback on linear time-invariant control systems.

Key words: security, resilient control, reachable set, robust control, ellipsoidal methods.

1 Introduction

The transition of modern infrastructures, such as chemical refineries, power plants, or manufacturing facilities, to computer-based technologies for supervisory control and data transmission has revealed significant challenges in the security of such cyber-physical systems (CPS), despite the numerous benefits it has provided in terms of efficiency, performance, and reliability. In the past, adaptive, robust, and stochastic control techniques have focused on rejecting *physical* disturbances, noise, and uncertainties, often striking a necessary balance between performance and robustness. However, with the migration of control system implementations to computer-based Ethernet networks, control design must deal with a new class of adversarial uncertainty injected from the *cyber* layer. The presence of these “attacks” introduce a new dimension to consider when designing control systems. Due to their strategic nature and intent to harm, developing design tools to harden control systems against such cyber attacks is essential for the safe operation of these critical infrastructures.

The concept of Resilient Control introduces the notion of control design in the presence of an attack or other

uncertain cyber environment [1,2]. The goal of a resilient control design is to protect the system from the risks induced by malicious signals delivered to the physical process through the cyber layer. In general, resilient control is characterized by a trade off between security and robustness, emphasizing that a system can be fragile and weak against cyber perturbations despite being robust against physical uncertainties [2,3]. In this context, *robustness* refers to the performance of the system under physical uncertainties and disturbances and *security* refers to the safety of the system against malicious signals and uncertainties entering from the cyber layer. Recent work in this theme includes studying the characteristics of defining resilient estimation schemes on the context of compromised sensors [4,5], or networked control systems for the trade off between a specific performance criteria like robustness in dynamic connectivity management, robustness for redundancy of direct information exchange and network’s asymptotical and exponential stability versus the network’s safety and security, [6,7,8].

In this paper we introduce a computational framework based on ellipsoidal geometric tools to quantify the security of a control system by the potential impact that a cyber attacks could have. We couple these tools with methods to quantify the robustness through an Output Covariance Constrained (OCC) $\|H\|_2$ gain between noise and output. Subject to a desired level of robustness, we formulate optimizations (with closed-form derivatives) to select the resilient observer and controller gains to

[★] The authors are with the Departments of Mechanical and Systems Engineering at the University of Texas at Dallas.

Email addresses: nxh150030@utdallas.edu (Navid Hashemi), jruths@utdallas.edu (Justin Ruths).

yield minimal impact due to attacks. These tools are also able to characterize the trade off between robustness and security through different control designs highlighting, in particular, that giving up a small amount of robustness can lead to large gains in security.

There is a mature line of control theoretic work surrounding the notion of robustness, see e.g., [9,10], but metrics for security are much less well-developed. In the past few years, the idea of using the set of states reachable by an attacker as a metric for security has emerged [11,12,13,14]. This reachable set quantifies the impact that attacks can have on the system state - the smaller the possible impact, the greater the security. Some work has leveraged these reachable sets to provide a more exacting notion of safety by quantifying the distance to states labeled as unsafe [15,13]. Here, we model attacks as additive perturbations affecting sensors measurements and are propagated to the system dynamics through output-based controllers. Therefore, we use the reachable set of the attack as our measure of impact and attempt to design the system in order to minimize the size of this reachable set.

The main idea of this paper is that we characterize the noise and attack as ellipsoidally bounded inputs, defined as $\mathcal{E}(Q_i)$, (see our work in [16]), to quantify the impact (reachable set) of the attack and use this framework to design the observer and controller gains L and K for observer-based feedback to minimize the attack impact. In this work, we first develop and update a recursive algorithm proposed in [17] to a one step formula on the geometric sum of several ellipsoidal sets. This allows us to use the result as part of the optimization to design the observer and controller gains to minimize the impact. In addition, we have also presented a novel formula to compute the exact boundary of the reachable set.

We publish this article alongside a companion paper, which studies the same problem using different tools [14]. Instead of using geometric tools to bound the reachable set, we use Lyapunov-type functions to derive ellipsoidal bounds on the reachable set. The advantage of the companion paper is that its approach - which has to-date been the dominant approach, see e.g., [16,13] - yields linear matrix inequalities (LMIs) that must be satisfied to find ellipsoidal bounds. These LMIs can be linearized and incorporated in efficient convex optimization problems. As we demonstrate in this paper, the convenience of these LMI solutions come at the cost of greater conservatism, which ultimately leads to a less-accurate trade off between robustness and security.

In [13], the authors also consider a similar problem. The approach is distinguished in three ways: (1) they design a dynamic output feedback controller and the independence of the controller matrices from the observer gain (the estimator is used for detection, not for feedback) makes the problem marginally easier to linearize; (2)

they consider a distributionally robust $\|H\|_\infty$ constraint for performance, in the sense that it does not incorporate information about the noise distributions; and (3) they do not focus on characterizing the trade off inherent between robustness and security.

Most notation of the paper is standard. The notation $\mathbb{V}^{n \times n}$ denotes the space of positive definite matrices of size n . We use $\bar{i}, \bar{j} := i, i+1, \dots, j-1, j$ to denote an interval of integers. The single entry matrix J_A^{ij} is a matrix of all zeros with the same size as matrix A whose (i, j) entry is a one ($[J_A^{ij}]_{ij} = 1$).

2 Background

The system we consider is a discrete time stochastic linear time-invariant (LTI) system with estimate feedback and zero mean Gaussian sensor and process noises with known covariances,

$$x_{k+1} = Fx_k + Gu_k + \nu_k, \quad (1)$$

$$y_k = Cx_k + \eta_k, \quad (2)$$

where the state $x_k \in \mathbb{R}^n$, $k \in \mathbb{N}$, evolves due to the state update provided by the state matrix $F \in \mathbb{R}^{n \times n}$, the control input $u_k \in \mathbb{R}^m$ filtered by the input matrix $G \in \mathbb{R}^{n \times m}$, and the Gaussian process noise $\nu_k \sim \mathcal{N}(0, R_1)$ where $R_1 \in \mathbb{V}^{n \times n}$. The output $y_k \in \mathbb{R}^p$ aggregates a linear combination, given by the observation matrix $C \in \mathbb{R}^{p \times n}$, of the states and the Gaussian sensor noise $\eta_k \sim \mathcal{N}(0, R_2)$ where $R_2 \in \mathbb{V}^{p \times p}$. In addition we assume that state matrix F is stable, the pair (F, C) is detectable and (F, G) is stabilizable.

In this work, we consider the scenario where the actual measurement y_k can be corrupted by an additive attack, $\delta_k \in \mathbb{R}^p$. At some point during the course of measurement and transmission of the output to the controller, the attack appears in the output signal, therefore the attacked output becomes

$$\bar{y}_k = y_k + \delta_k = Cx_k + \eta_k + \delta_k. \quad (3)$$

If the attacker has access to the measurements, then it is possible for the attack δ_k to cancel some or all of the original measurement y_k , so an additive attack can achieve arbitrary control over the “effective” output of the system.

Because our system is stochastic and all states are, in general, not observed, we employ an estimator to produce a prediction of the system behavior

$$\hat{x}_{k+1} = F\hat{x}_k + Gu_k + L(\bar{y}_k - C\hat{x}_k), \quad (4)$$

where $\hat{x}_k \in \mathbb{R}^n$ is the estimated state and the observer gain L is designed to force system states to track the estimated states. This estimate is used for observer-based

output feedback,

$$u_k = K\hat{x}_k, \quad (5)$$

where $K \in \mathbb{R}^{m \times n}$ denotes the controller gain matrix. Since typically system characteristics cannot be modified, it is the observer and controller gains L and K that give designers the ability to shape the performance of the system, such as for stability (e.g., pole placement) and robustness (e.g., H_∞). In this paper we develop tools to design L and K to limit the impact of attacks on control systems.

Knowing the output may be corrupted, system operators implement a model-based detector to identify anomalies in the behavior of the system. Such detectors take, as input, the sequence of residuals r_k ,

$$r_k = \bar{y}_k - C\hat{x}_k, \quad (6)$$

which is the difference between what we actually receive (\bar{y}_k) and expect to receive ($C\hat{x}_k$), which evolves according to

$$x_{k+1} = (F + GK)x_k - GKe_k + \nu_k \quad (7)$$

$$e_{k+1} = (F - LC)e_k - L\eta_k + v_k - L\delta_k, \quad (8)$$

$$y_k = Cx_k + \eta_k + \delta_k, \quad (9)$$

$$r_k = Ce_k + \eta_k + \delta_k, \quad (10)$$

where $e_k = x_k - \hat{x}_k$ is the estimation error. In the absence of attacks (i.e., $\delta_k = 0$), we can show that in steady-state the r_k random variable has covariance

$$\begin{aligned} \Sigma &= \mathbf{E}[r_k r_k^T] = C\mathbf{E}[e_k e_k^T]C^T + \mathbf{E}[\eta_k \eta_k^T], \\ &= CP_e C^T + R_2, \end{aligned} \quad (11)$$

where the steady state covariance of the estimation error $P_e = \lim_{k \rightarrow \infty} P_k = \mathbf{E}[e_k e_k^T]$ is

$$\begin{aligned} P_e &= \mathbf{E}[e_k e_k^T] \\ &= (F - LC)\mathbf{E}[e_k e_k^T](F - LC)^T \\ &\quad + LE[\eta_k \eta_k^T]L^T + \mathbf{E}[\nu_k \nu_k^T], \\ &= (F - LC)P_e(F - LC)^T + LR_2L^T + R_1. \end{aligned} \quad (12)$$

Here, we consider the chi-squared detector, although similar analysis can be done with other detector choices [18,19]. In the case of the chi-squared detector, a quadratic distance measure z_k is created to be sensitive to changes in the variance of the distribution as well as the expected value,

$$z_k = r_k^T \Sigma^{-1} r_k. \quad (13)$$

The chi-squared detector generates alarms when the distance measure exceeds a threshold $\alpha \in \mathbb{R}_{>0}$

$$\begin{cases} z_k \leq \alpha & \longrightarrow \text{no alarm,} \\ z_k > \alpha & \longrightarrow \text{alarm: } k' = k, \end{cases} \quad (14)$$

such that alarm time(s) k' are produced. The Σ^{-1} factor in the definition of z_k re-scales the distribution ($\mathbf{E}[z_k] = p$, $\mathbf{E}[z_k z_k^T] = 2p$) so that the threshold α can be designed independent of the specific statistics (mean and covariance) of the noises ν_k and η_k ; instead, it can be selected simply based on the number of sensors, p . Typically a false alarm rate is chosen and α is then computed using the cumulative distribution function of the chi-square distribution, the regularized lower incomplete gamma function [18].

2.1 Definition of attack

Detectors are designed to identify anomalies in the system, and limit what the attacker is able to accomplish if he/she wants to remain undetected. We consider a worst-case deterministic attack in which the attacker wishes to raise no detector alarms. While more sophisticated attacks exist, the deterministic nature of this attack type make it a ready benchmark for comparison of the tools we develop in this paper compared with existing methods that leverage convex optimization [16,14]. This attack model requires strong knowledge of and access to the system dynamics, statistics of noises, output of the observer (\hat{x}_k), and chi-squared detector threshold. The goal of this stealthy attack is to construct the worst case scenario for attack impact while remaining stealthy to the detector.

Zero-alarm attacks employ attack sequences that maintain the distance measure at or below the threshold, i.e., $z_k \leq \alpha$. These attacks generate no alarms during the attack. To satisfy this condition we define the attack as

$$\delta_k = \Sigma^{\frac{1}{2}} \bar{\delta}_k - (\bar{y}_k - C\hat{x}_k) = -Ce_k - \eta_k + \Sigma^{\frac{1}{2}} \bar{\delta}_k, \quad (15)$$

where $\bar{\delta}_k \in \mathbb{R}^p$ is any vector such that $\bar{\delta}_k^T \bar{\delta}_k \leq \alpha$ and $\Sigma^{\frac{1}{2}}$ is the symmetric square root of Σ (recall the attacker has read access to the sensor, y_k , and knowledge of the estimate, \hat{x}_k). From (15),

$$\begin{aligned} z_k &= r_k^T \Sigma^{-1} r_k \\ &= (Ce_k + \eta_k + \delta_k)^T \Sigma^{-1} (Ce_k + \eta_k + \delta_k) \\ &= (\Sigma^{\frac{1}{2}} \bar{\delta}_k)^T \Sigma^{-1} (\Sigma^{\frac{1}{2}} \bar{\delta}_k) \end{aligned} \quad (16)$$

$$= \bar{\delta}_k^T \bar{\delta}_k \leq \alpha. \quad (17)$$

Since $z_k \leq \alpha$, no alarms are raised. We will show later (see Remark 2) that our optimization becomes independent of the specific value of α . This implies that our optimization finds optimal observer and controller gains to limit attacker impact whether the attacker aims to be stealthy or non-stealthy, thus actually considering a broader class of attacks than simply zero-alarm attacks.

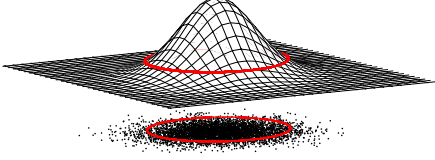


Figure 1. The \bar{p} -probable ellipsoid captures a level set of the distribution of Gaussian noise, such that drawing a sample within the ellipsoid occurs with probability \bar{p} and drawing a sample the falls outside the ellipsoid occurs with probability $1 - \bar{p}$. Typically \bar{p} is chosen close to 1.

2.2 Truncating Noise Distributions

The tools we use in this paper to measure the attack impact quantify the size of the set of states reachable by the inputs of the system, namely the attack input and the noise inputs. A system (even a stable system) driven by (unbounded) Gaussian noise has an unbounded reachable set - while the probability of having a very large state may be vanishingly small, it is still nonzero. In order to get a practical sense of the attack impact (as a finite reachable set), it is standard to truncate the noise at some confidence level. We will show later (see Remark 2) that our optimization of observer and controller gains is independent of the choice of this truncation level. This implies that the optimal gains minimize the impact of the attacker solely as a function of the covariances of the noise and not the truncation bound we select.

In the absence of an attack, the system is driven by zero-mean Gaussian noises with infinite support. Truncating these multivariate distributions can be done with ellipsoidal sets, which are effectively level-sets of the probability density functions such that drawing a noise sample falling outside this ellipsoidal set occurs with probability $1 - \bar{p}$ (see Figure 1), i.e.,

$$\Pr(\nu_k^T R_1^{-1} \nu_k \leq \bar{\nu}) = \bar{p}, \quad (18)$$

$$\Pr(\eta_k^T R_2^{-1} \eta_k \leq \bar{\eta}) = \bar{p}, \quad (19)$$

for the system and measurement noise, respectively (the values $\bar{\nu}$ and $\bar{\eta}$ are called Mahalanobis distances; \bar{p} could be chosen differently for each distribution, but for simplicity we consider them the same).

By truncating the noises at their Mahalanobis distances, we can then consider each of the noises as ellipsoidally bounded random inputs, i.e., $\nu_k \in \mathcal{E}(\bar{\nu} R_1)$ and $\eta_k \in \mathcal{E}(\bar{\eta} R_2)$, where

$$\mathcal{E}(R, c) = \{ \xi \mid (\xi - c)^T R^{-1} (\xi - c) \leq 1 \}, \quad (20)$$

with $R \in \mathbb{V}$ called the shape matrix and c the center of the ellipsoid. When the center is the origin, we often drop the second argument, $\mathcal{E}(R) = \mathcal{E}(R, 0)$.

2.3 Reachable Set

The fact that the attack $\bar{\delta}_k$ is contained within a sphere with nonzero volume, $\bar{\delta} \in \mathcal{E}(\alpha I)$, indicates the attacker is capable of having an effect on the system while still remaining stealthy to the detector. In order to quantify the impact of this stealthy attack, we require a metric, and a popular choice is the set of states reachable by the action of the attack.

Applying the structure of the zero-alarm attack (15) to (7), the evolution of the system dynamics can be written as a function of the two inputs ν_k and $\bar{\delta}_k$ (recall η_k is effectively canceled in the definition of δ_k in (15)),

$$e_{k+1} = F e_k - L \Sigma^{\frac{1}{2}} \bar{\delta}_k + \nu_k, \quad (21)$$

$$x_{k+1} = (F + GK) x_k - GK e_k + \nu_k. \quad (22)$$

In steady state, (21) and (22) become (for $k \geq 2$),

$$e_k = \sum_{i=1}^{k-1} F^i \nu_{k-i} - F^i L \Sigma^{\frac{1}{2}} \bar{\delta}_{k-i}, \quad (23)$$

$$x_k = \sum_{i=1}^{k-1} F^i \nu_{k-i} + ((F + GK)^i - F^i) L \Sigma^{\frac{1}{2}} \bar{\delta}_{k-i}. \quad (24)$$

To highlight the contribution of each input on the dynamics, we can split (21) and (22) based on the contributions of ν_k and $\bar{\delta}_k$, where for the estimation error, $e_k = e_k^\nu + e_k^{\bar{\delta}}$, and for the state, $x_k = x_k^\nu + x_k^{\bar{\delta}}$,

$$e_{k+1}^\nu = F e_k^\nu + \nu_k, \quad (25)$$

$$x_{k+1}^\nu = (F + GK) x_k^\nu - GK e_k^\nu + \nu_k, \quad (26)$$

$$e_{k+1}^{\bar{\delta}} = F e_k^{\bar{\delta}} - L \Sigma^{\frac{1}{2}} \bar{\delta}_k, \quad (27)$$

$$x_{k+1}^{\bar{\delta}} = (F + GK) x_k^{\bar{\delta}} - GK e_k^{\bar{\delta}}. \quad (28)$$

Now that we have solved for x_k in (24), we can start to compute the geometry of its reachable set, which shows the ability of the attack to change the system state. Equation (24) shows that the overall state involves ellipsoidally bounded random variables $\bar{\delta}_k$ and ν_k . In the following sections of this paper we show how to generate the zero-alarm reachable state set exploiting the independence and ellipsoidal boundedness of these random variables. We use the geometric sum to explore all of the states x_k that are possible through all the different realizations of ν_i and $\bar{\delta}_i$ over $i \in \bar{1}, k-1$.

Definition 1 [20] *The geometric (or Minkowski) sum of two convex sets $\mathcal{S}_1, \mathcal{S}_2 \subset \mathbb{R}^n$ is*

$$\mathcal{S}_1 \oplus \mathcal{S}_2 = \left\{ s_1 + s_2 \mid s_1 \in \mathcal{S}_1, s_2 \in \mathcal{S}_2 \right\}. \quad (29)$$

Note that while the geometric sum of two ellipsoids is a convex set, it is in general not an ellipsoid.

Lemma 1 [20] *Given vector $x \in \mathcal{E}(Q, c)$, with shape matrix $Q \in \mathbb{V}^{n \times n}$ and mean value $c \in \mathbb{R}^n$, then for any linear mapping $T(x) = Ax$ with $A \in \mathbb{R}^{n \times n}$ the vector $\xi = T(x) = Ax$ lies within an ellipsoid with shape matrix AQA^T and mean value Ac , i.e., $\xi \in \mathcal{E}(AQA^T, Ac)$.*

For the state dynamics, this geometric sum is denoted by $\mathcal{R}_{x,k}$ and based on (24),

$$\mathcal{R}_{x,k} = \mathcal{R}_{x,k}^\nu \oplus \mathcal{R}_{x,k}^\delta, \quad (30)$$

where in steady state $\mathcal{R}_{x,k}^\nu$ denotes the the process noise contribution governed by (26), and $\mathcal{R}_{x,k}^\delta$ denotes the attack input contribution governed by (28),

$$\mathcal{R}_{x,k} = \bigoplus_{i=0}^k \bar{\nu} F^i R_1 F^{iT} \oplus \alpha H_i L \Sigma L^T H_i^T, \quad (31)$$

with $H_i = (F + GK)^i - F^i$, and \oplus denotes geometric sum and \bigoplus denotes geometric series.

In its current form, (31) is convenient, however, remains abstract. The next section of this paper develops tools to analytically quantify and bound this chain of geometric sums so that we can incorporate them into an optimization to minimize this attack-induced reachable set.

3 Ellipsoidal Approximation of the Reachable Set

It is important to observe that even though each term of the geometric sum in (31) is an ellipsoid, the overall geometric sum (and, therefore, the overall reachable set) is, in general, not an ellipsoid. Characterizing the exact boundary of the k -step reachable set has not appeared in the literature, and here we capture this in Theorem 1 in Section 3.1. While characterizing the exact boundary provides a precise picture of the reachable set, due to the iterative nature of its construction, optimizing the reachable set directly, such as through designing the observer and controller gain matrices L and K , would generally require blackbox optimization strategies. This motivates us to construct an ellipsoidal approximation of the reachable set, which is more easily integrated into further calculation and optimization.

3.1 Ellipsoidal Approximation of a Geometric Sum

A central tool in working with geometric operations on convex sets is the support function,

$$\rho(\ell|\mathcal{H}) = \sup_{x \in \mathcal{H}} \langle \ell, x \rangle, \quad (32)$$

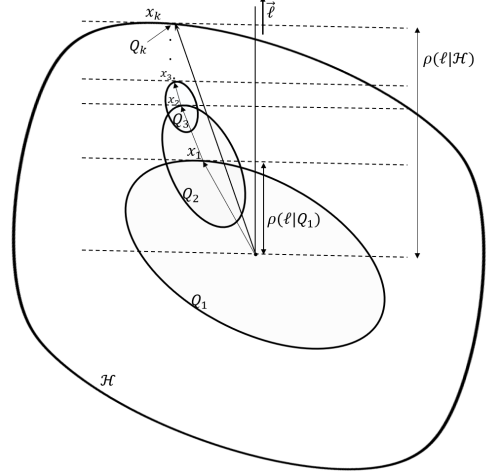


Figure 2. Convex set \mathcal{H} as a geometric sum of k ellipsoids. Here the ellipsoids are decreasing in size as would be the case for a stable system and ellipsoids generated by (31).

which can be interpreted as the largest projection of elements of the convex set \mathcal{H} onto the direction given by the unit vector ℓ . Containment of one convex set within another convex set, $\mathcal{H} \subset \mathcal{S}$, is exactly captured by the support function of the contained set being less than or equal to the support function of the containing set over all choices of ℓ ,

$$\rho(\ell|\mathcal{H}) \leq \rho(\ell|\mathcal{S}), \quad \forall \ell \in \mathbb{R}^n. \quad (33)$$

In addition, the support function of a geometric sum of two convex sets can be expressed as the sum of their support functions [17]. The geometric sum of k ellipsoids centered at zero with shape matrices Q_1, \dots, Q_k (see Figure 2) is then

$$\rho(\ell|\mathcal{H}) = \sum_{i=1}^k \rho(\ell|\mathcal{E}(Q_i)). \quad (34)$$

When the convex sets of interest are ellipsoids, the support function can further be expressed as

$$\rho(\ell|\mathcal{E}(Q)) = \langle \ell, Q\ell \rangle^{\frac{1}{2}}. \quad (35)$$

Therefore, the geometric sum (34) can be written as

$$\rho(\ell|\mathcal{H}) = \sum_{i=1}^k \langle \ell, Q_i \ell \rangle^{\frac{1}{2}}. \quad (36)$$

The following result provides a closed form formula to calculate the exact geometric sum of a finite collection of ellipsoids based on their support functions.

Theorem 1 *Consider the set of k ellipsoids characterized by the positive definite matrices $Q_i \in \mathbb{V}^{n \times n}$, $i \in \{1, \dots, k\}$.*

The exact convex shape of their geometric sum is

$$\mathcal{H} = \bigoplus_{i=1}^k \mathcal{E}(Q_i) = \left\{ x = \sum_{i=1}^k \langle \ell, Q_i \ell \rangle^{-\frac{1}{2}} Q_i \ell \mid \|\ell\| \leq 1 \right\}. \quad (37)$$

The boundary $\partial\mathcal{H}$ of the convex set is found when $\|\ell\| = 1$.

Proof: One way to interpret the support function (32) is that ℓ provides the normal vector of the hyperplane that is tangent to the convex set \mathcal{H} at the point x . By the definition of the geometric sum, the boundary point x can be written as the sum of elements $x_i \in \mathcal{E}(Q_i)$ for $i \in \overline{1, k}$,

$$x = \sum_{i=1}^k x_i, \quad (38)$$

where each x_i is a boundary point on each individual ellipsoid, i.e., the maximizer of

$$\rho(\ell \mid \mathcal{E}(Q_i)) = \sup_{\xi \in \mathcal{E}(Q_i)} \langle \ell, \xi \rangle, \quad (39)$$

analogous to (32). Hence, for each $i \in \overline{1, k}$, ℓ provides the (unit) normal vector of the hyperplane that is tangent to the ellipsoid $\mathcal{E}(Q_i)$ at the point x_i . The normal vector of the ellipsoid can also be expressed as the gradient of the level set $x_i^T Q_i^{-1} x_i = 1$, hence,

$$\ell = \frac{\nabla(x_i^T Q_i^{-1} x_i - 1)}{\|\nabla(x_i^T Q_i^{-1} x_i - 1)\|} = \frac{Q_i^{-1} x_i}{\sqrt{x_i^T Q_i^{-2} x_i}}. \quad (40)$$

If we use again the fact that $x_i^T Q_i^{-1} x_i = 1$,

$$\begin{aligned} \ell &= \frac{(x_i^T Q_i^{-1} x_i) Q_i^{-1} x_i}{\sqrt{x_i^T Q_i^{-2} x_i}} = x_i^T \frac{Q_i^{-1} x_i}{\sqrt{x_i^T Q_i^{-2} x_i}} Q_i^{-1} x_i \\ &= x_i^T \ell Q_i^{-1} x_i. \end{aligned} \quad (41)$$

Note that as the maximizer of (39), the projection of x_i onto ℓ gives the support function,

$$x_i^T \ell = \rho(\ell \mid \mathcal{E}(Q_i)) = \langle \ell, Q_i \ell \rangle^{\frac{1}{2}}. \quad (42)$$

Substituting (42) into (41) yields

$$\ell = \langle \ell, Q_i \ell \rangle^{\frac{1}{2}} Q_i^{-1} x_i. \quad (43)$$

Finally, solving for x_i and plugging these into (38) completes the proof. \blacksquare

As mentioned previously, working with the convex set \mathcal{H} directly is challenging because for large enough k it can be quite complicated and quantifying properties of the exact set is difficult. In addition its dependence on

ℓ makes it troublesome to compute the derivatives required for optimizing the set. Theorem 2 characterizes the family of shape matrices that provide an outer ellipsoidal bound on the exact convex set, i.e., $\mathcal{H} \subseteq \mathcal{E}(Q)$. This result is similar to Theorem 2.7.1 in [17], which computes the geometric sum of k ellipsoids through pairwise sums. The recursive approach in [17] approximates the geometric sum of two ellipsoids with an ellipsoid on each iteration which fundamentally restricts the choice of the outer bound and does not provide any guarantees on the tightness of the bound.

Theorem 2 Consider the set of k ellipsoids characterized by the positive definite matrices $Q_i \in \mathbb{V}^{n \times n}$, $i \in \overline{1, k}$. The ellipsoid $\mathcal{E}(Q)$ is an outer bound of their geometric sum $\mathcal{H} = \bigoplus_{i=1}^k \mathcal{E}(Q_i)$, i.e., $\mathcal{H} \subseteq \mathcal{E}(Q)$, if,

$$Q = \sum_{i=1}^k Q_i + \sum_{i,j \in \mathcal{I}} p_{ij} Q_i + p_{ij}^{-1} Q_j \quad (44)$$

where $p_{ij} > 0 \forall (i, j) \in \mathcal{I} = \{(i, j) \mid 1 \leq i < j \leq k, i, j \in \overline{1, k}\}$.

Proof: To prove that the convex set of the geometric sum is bounded by the ellipsoid, i.e., $\mathcal{H} \subseteq \mathcal{E}(Q)$, it suffices to prove (33) holds between the support functions $\rho(\ell \mid \mathcal{E}(Q))$ and $\rho(\ell \mid \mathcal{H})$. We first define a positive coefficient p_{ij} between the shape matrices Q_i and Q_j and in order to avoid redundancy assume $i < j$ which constructs the set \mathcal{I} . Given a unit vector ℓ , we start with the following sum of squares which is always nonnegative

$$\sum_{i,j \in \mathcal{I}} \left(\sqrt{p_{ij}} \langle \ell, Q_i \ell \rangle^{\frac{1}{2}} - \sqrt{p_{ij}^{-1}} \langle \ell, Q_j \ell \rangle^{\frac{1}{2}} \right)^2 \geq 0.$$

Expanding this series results in,

$$\sum_{i,j \in \mathcal{I}} (p_{ij} \langle \ell, Q_i \ell \rangle + p_{ij}^{-1} \langle \ell, Q_j \ell \rangle) \geq \sum_{i,j \in \mathcal{I}} 2 \langle \ell, Q_i \ell \rangle^{\frac{1}{2}} \langle \ell, Q_j \ell \rangle^{\frac{1}{2}},$$

and adding $\sum_{i=1}^k \langle \ell, Q_i \ell \rangle$ to both sides of the inequality,

$$\begin{aligned} & \sum_{i=1}^k \langle \ell, Q_i \ell \rangle + \sum_{i,j \in \mathcal{I}} p_{ij} \langle \ell, Q_i \ell \rangle + p_{ij}^{-1} \langle \ell, Q_j \ell \rangle \\ & \geq \sum_{i=1}^k \langle \ell, Q_i \ell \rangle + \sum_{i,j \in \mathcal{I}} 2 \langle \ell, Q_i \ell \rangle^{\frac{1}{2}} \langle \ell, Q_j \ell \rangle^{\frac{1}{2}}. \end{aligned}$$

allows us to complete the square on the right hand side of the inequality. The left hand side, then, becomes the definition of Q in (44), such that it is equal to $\langle \ell, Q \ell \rangle$.

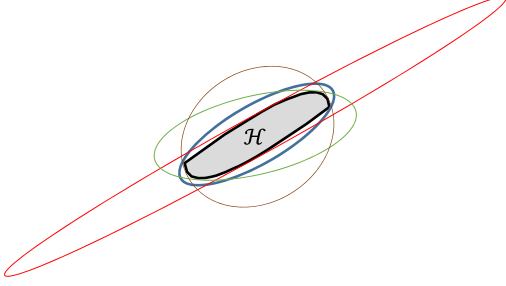


Figure 3. There are an infinite number of ellipsoids that are a tight outer bound of the convex set \mathcal{H} , each tangent to \mathcal{H} at different points (alternatively corresponding to different choices of the unit vector ℓ). A careful choice of these tangent points provides a useful outer bound.

Therefore, $\langle \ell, Q\ell \rangle \geq \left(\sum_{i=1}^k \langle \ell, Q_i \ell \rangle^{\frac{1}{2}} \right)^2$, which means,

$$\underbrace{\langle \ell, Q\ell \rangle^{\frac{1}{2}}}_{\rho(\ell | \mathcal{E}(Q))} \geq \underbrace{\sum_{i=1}^k \langle \ell, Q_i \ell \rangle^{\frac{1}{2}}}_{\rho(\ell | \mathcal{H})}, \quad (45)$$

and the underbrace definitions come from (35) and (36). We conclude then that $\mathcal{H} \subseteq \mathcal{E}(Q)$ from (33). ■

Remark 1 Although it is written in several terms in (44), the shape matrix Q is a linear combination of the individual shape matrices Q_i , $Q = \sum_{i=1}^k \alpha_i Q_i$, with coefficients α_i that are the combination of p_{ij} and p_{ij}^{-1} . If the coefficients of the Q_i are large, then it makes $\mathcal{E}(Q)$ a large and loose outer bound on \mathcal{H} . This occurs when p_{ij} is either very large or very small (so p_{ij}^{-1} is large). Thus to have a tight outer bound, which is tangent to the exact sum \mathcal{H} , the challenge is to select the definition of p_{ij} appropriately.

3.2 Tight Ellipsoidal Approximations

Theorem 2 characterizes the family of ellipsoids that out-bound the reachable set, including both tight and conservative overapproximations of the reachable set. The inequality in (45) becomes an equality if $\mathcal{E}(Q)$ touches the convex set \mathcal{H} in the direction of the unit vector ℓ - i.e., is a tight approximation - and occurs when p_{ij} is selected appropriately. There are an infinite number of such tight ellipsoidal bounds (see Figure 3) and we will show throughout this paper the advantages of the minimum trace ellipsoidal bound. We denote this minimum trace ellipsoid by $\mathcal{E}(Q^*)$.

This ellipsoid provides analytic tractability for the computation of its shape matrix which is derived in Lemma 2. In Section 5 where we design the controller and observer gains, this selection also makes the subsequent optimization to minimize the attack reachable set independent of the noise (truncation level and distribution).

Lemma 2 Consider the set of k ellipsoids characterized by the positive definite matrices $Q_i \in \mathbb{V}^{n \times n}$, $i = 1, k$. The ellipsoid $\mathcal{E}(Q^*)$ is a tight outer bound of their geometric sum $\mathcal{H} = \bigoplus_{i=1}^k \mathcal{E}(Q_i)$, i.e., $\mathcal{H} \subseteq \mathcal{E}(Q^*)$, where

$$Q^* = \left(\sum_{i=1}^k \sqrt{\text{tr}(Q_i)} \right) \left(\sum_{i=1}^k \frac{Q_i}{\sqrt{\text{tr}(Q_i)}} \right). \quad (46)$$

Specifically, of all the shape matrices that correspond to ellipsoid outer bounds of \mathcal{H} , Q^* has the minimum trace.

Proof: Starting from the general condition on p_{ij} for $\mathcal{E}(Q)$ to be an outer bound, (44), we take the trace operation of both sides

$$\text{tr}(Q) = \sum_{i=1}^k \text{tr}(Q_i) + \sum_{i,j \in \mathcal{I}} p_{ij} \text{tr}(Q_i) + p_{ij}^{-1} \text{tr}(Q_j) \quad (47)$$

This makes $\text{tr}(Q)$ a function of p_{ij} , $(i, j) \in \mathcal{I}$. To find the minima, we find the stationary points of $\text{tr}(Q)$ with respect to p_{ij} ,

$$\frac{\partial \text{tr}(Q)}{\partial p_{ij}} = \text{tr}(Q_i) - \frac{\text{tr}(Q_j)}{p_{ij}^2} = 0. \quad (48)$$

with the laplacian always positive due to the positive definiteness of each Q_1, \dots, Q_k shape matrices,

$$\nabla^2 \text{tr}(Q) = \text{diag} \left[\left\{ \frac{2\text{tr}(Q_j)}{p_{ij}^3} \right\}_{(i,j) \in \mathcal{I}} \right] > 0, \quad (49)$$

where the pairs (i, j) are ordered first by i and then by j . The solution of (48) is $p_{ij}^* = \sqrt{\text{tr}(Q_j)/\text{tr}(Q_i)}$, which is unique due to the positive laplacian implying a global minimum. Boundedness of the reachable set (see Section 3.3) guarantees the existence of the solution for optimal values p_{ij}^* . Substituting this choice of p_{ij} into (44) completes the proof. ■

Our choice of the minimum trace ellipsoid differs from the more common choice of tight ellipsoidal shape matrix [17,20],

$$Q = \left(\sum_{i=1}^k \langle \ell, Q_i \ell \rangle^{\frac{1}{2}} \right) \left(\sum_{i=1}^k \langle \ell, Q_i \ell \rangle^{-\frac{1}{2}} Q_i \right), \quad (50)$$

which emerges from an iterative approach to approximating the k step Minkowski sum of ellipsoids. In the context of our more general Theorem 2, we see that this corresponds to the choice,

$$p_{ij} = \frac{\langle \ell, Q_j \ell \rangle^{\frac{1}{2}}}{\langle \ell, Q_i \ell \rangle^{\frac{1}{2}}} = \frac{\rho(\ell | \mathcal{E}(Q_j))}{\rho(\ell | \mathcal{E}(Q_i))}, \quad \forall i, j \in \mathcal{I}. \quad (51)$$

Now we can see that one of the most important features of Theorem 2 (and therefore Lemma 2) is that it is able to drop the dependence on the unit vector ℓ , which is a user-specified choice. Keeping ℓ involved, as in (50)-(51), makes it difficult to generalize the analysis and take analytic derivatives of the shape matrix in terms of the gain matrices (in Section 5). The following result confirms that this choice of p_{ij} corresponding to the family of shape matrices given by (50) does not, in general, capture the minimum trace shape matrix in Lemma 2.

Lemma 3 *Consider the set of k ellipsoids characterized by shape matrices $Q_i \in \mathbb{V}^{n \times n}$, $i \in \overline{1, k}$ where d of these shape matrices are linearly independent. Let \mathcal{Q} be the set of matrices specified by (50) over all choices of $\ell \in \mathbb{R}^n$. If $d > n$, then $Q^* \notin \mathcal{Q}$, where Q^* is the shape matrix of the minimum trace ellipsoid that contains the geometric sum $\mathcal{H} = \bigoplus_{i=1}^k \mathcal{E}(Q_i)$.*

The proof of Lemma 3 is provided in Appendix A. Note that in our context k is typically relatively large and so typically $d > n$.

3.3 A Tight Ellipsoidal Bound on the Reachable Set

The expression of the reachable set in (31) indicates that the reachable set of the system state is a function of time, k , and composed of contributions from both the noise and the attack. The noise-driven portion of the system is characterized by ellipsoids with shape matrices $Q_i^\nu = \bar{\nu} F^i R_1 F^{iT}$; the attack-driven portion is characterized by ellipsoids with shape matrices $Q_i^\delta = \alpha H_i L \Sigma L^T H_i^T$, with $H_i = (F + GK)^i - F^i$. Using the framework built above, the reachable set $\mathcal{R}_{x,k} \subseteq \mathcal{E}(Q_k^*)$, where Q_k^* is given by Lemma 2 with $\{Q_i\}_{i=0}^k = \{Q_i^\nu, Q_i^\delta\}_{i=0}^k$ (note we introduce the subscript k to Q^* here to explicitly indicate the dependence on time).

The stability of the open-loop (F) and closed-loop ($F + GK$) dynamics along with the bounded inputs ν_k and δ_k imply that the set of reachable states is bounded. In Appendix B, we use these facts to also show that the minimum trace ellipsoidal outer bound is also bounded. In particular, we show that the sequence $\{Q_k^*\}$ is Cauchy, which suggests there exists a k^* that satisfies an arbitrary level of approximation accuracy,

$$\left\| Q_{k^*}^* - \lim_{k \rightarrow \infty} Q_k^* \right\| \leq \epsilon. \quad (52)$$

This k^* can be interpreted as the settling time of the system. Thus, up to some ϵ -accuracy, the infinite horizon reachable set $\mathcal{R}_x \subseteq \mathcal{E}(Q^*)$, where $Q^* = \lim_{k \rightarrow \infty} Q_k^*$

$$Q^* = \left(\sum_{i=0}^{k^*} \sqrt{\alpha \text{tr}(H_i L \Sigma L^T H_i^T)} + \sqrt{\bar{\nu} \text{tr}(F^i R_1 F^{iT})} \right) \times \left(\sum_{i=0}^{k^*} \frac{\alpha H_i L \Sigma L^T H_i^T}{\sqrt{\text{tr}(\alpha H_i L \Sigma L^T H_i^T)}} + \frac{\bar{\nu} F^i R_1 F^{iT}}{\sqrt{\text{tr}(\bar{\nu} F^i R_1 F^{iT})}} \right). \quad (53)$$

Beyond simply quantifying the reachable set, the goal of this paper is to design the observer and controller gain matrices to minimize the reachable set by minimizing the ellipsoid $\mathcal{E}(Q^*)$.

From (53) but even more clearly from (23)-(24), there is a set of trivial choices of L and K that minimize the ellipsoidal bound and, therefore, the reachable set. In general, $K = 0$ or $L = 0$ are always included in the set of trivial solutions regardless of the properties of F and G (see Appendix C for complete characterization of the trivial set). Either of these choices ($L = 0$ or $K = 0$) effectively cuts the feedback loop for both the attacker and controller. Hence while these trivial choices eliminate the impact of the attack on the reachable set, it also removes the influence of the feedback controller, and we cannot guarantee the performance of the control system design, such as rate of stability, overshoot, and robustness. Work in resilient control has already identified the trade off between security and other metrics, so it is expected that similar exchanges are relevant to the design of observer and controller gains. To avoid these trivial solutions and to explore the implied trade off, we additionally require a performance criteria to be satisfied. Here we propose a robustness characteristic quantified by an output covariance constrained $\|H\|_2$ requirement.

4 Output Covariance Constrained (OCC) $\|H\|_2$ Constraint

A model-based attack detection approach already leverages knowledge of the system's noise characteristics (covariances), hence it is fitting to use this knowledge to find a more tailored robustness metric, which is why we use an Output Covariance Constrained (OCC) $\|H\|_2$ gain as the closed loop performance criteria [21]. We contrast this kind of choice with $\|H\|_2$ and $\|H\|_\infty$ definitions that do not take the input covariances into account and thus can be considered as "distributionally robust" gains from noise-to-output. The OCC $\|H\|_2$ gain, which bounds the measurement based on the covariance of input noises, constrains a given signal $h_k = H_1 x_k + H_2 \omega_k$ based on the input $\omega_k = [\nu_k^T, \eta_k^T]^T$. Here we select $h_k = y_k$, making $H_1 = C$, $H_2 = [0_{p \times n}, I_{p \times p}]$.

When there is no attack, the system evolves according to

$$x_{k+1} = (F + GK)x_k - GKe_k + \nu_k, \quad (54)$$

$$e_{k+1} = (F - LC)e_k + \nu_k - L\eta_k, \quad (55)$$

$$y_k = Cx_k + \eta_k, \quad (56)$$

or using the stacked state $\xi_k = [x_k^T, e_k^T]^T$,

$$\begin{aligned} \xi_{k+1} &= A\xi_k + B\omega_k, \\ y_k &= [C, 0] \xi_k + [0, I] \omega_k, \end{aligned} \quad (57)$$

with

$$A = \begin{bmatrix} F + GK & -GK \\ 0 & F - LC \end{bmatrix} \quad B = \begin{bmatrix} I & 0 \\ I & -L \end{bmatrix}. \quad (58)$$

The OCC $\|H\|_2$ criteria specifies the gain from the noise to the output should be less than a desired value $\bar{\gamma}$,

$$\lim_{N \rightarrow \infty} \sqrt{\frac{\frac{1}{N} \sum_{k=1}^N y_k^T y_k}{\frac{1}{N} \sum_{k=1}^N \omega_k^T \omega_k}} = \sqrt{\frac{\mathbf{E}[y_k^T y_k]}{\mathbf{E}[\omega_k^T \omega_k]}} \leq \bar{\gamma}. \quad (59)$$

Lemma 4 *Given the dynamics in (54)-(57), the Output Covariance Constrained $\|H\|_2$ constraint in (59) is satisfied if the steady state covariance, $\mathbf{P} \geq 0$,*

$$\mathbf{P} = \begin{bmatrix} \mathbf{P}_x & \mathbf{P}_{xe} \\ \mathbf{P}_{xe}^T & \mathbf{P}_e \end{bmatrix} = \lim_{k \rightarrow \infty} \mathbf{E}[\xi_k \xi_k^T], \quad (60)$$

satisfies the Lyapunov equation

$$\mathbf{P} = \mathbf{A}\mathbf{P}\mathbf{A}^T + \mathbf{R}, \quad \mathbf{R} = \begin{bmatrix} R_1 & R_1 \\ R_1 & R_1 + LR_2L^T \end{bmatrix}, \quad (61)$$

and the following inequality holds,

$$\begin{aligned} \mathcal{C}_{k^*} &= \text{tr}(E_x^T C^T C E_x \mathbf{P}) + \text{tr}(R_2) \\ &\quad - \bar{\gamma}^2 (\text{tr}(R_1) + \text{tr}(R_2)) \leq 0, \end{aligned} \quad (62)$$

where $E_x = [I_n, 0_{n \times n}]$.

Proof: From the definition of the output (56) and of ω_k , we can calculate the quadratic terms in (59),

$$y_k^T y_k = x_k^T C^T C x_k + 2x_k^T C^T \eta_k + \eta_k^T \eta_k, \quad (63)$$

$$\omega_k^T \omega_k = \nu_k^T \nu_k + \eta_k^T \eta_k. \quad (64)$$

Taking the expectation,

$$\begin{aligned} \mathbf{E}[y_k^T y_k] &= \mathbf{E}[x_k^T C^T C x_k] + \mathbf{E}[\eta_k^T \eta_k] \\ &= \text{tr}(C^T C \mathbf{E}[x_k x_k^T]) + \text{tr}(R_2), \end{aligned} \quad (65)$$

(recall x_k and η_k are independent) and similarly,

$$\mathbf{E}[\omega_k^T \omega_k] = \mathbf{E}[\nu_k^T \nu_k] + \mathbf{E}[\eta_k^T \eta_k] = \text{tr}(R_1) + \text{tr}(R_2). \quad (66)$$

The unknown quantity is then the covariance of the state, $\mathbf{E}[x_k x_k^T]$, which is the first block of the stacked state ξ_k covariance $\mathbf{P}_k = \mathbf{E}[\xi_k \xi_k^T]$. This covariance follows the update, evaluating $\mathbf{E}[\xi_{k+1} \xi_{k+1}^T]$ with

$$\mathbf{P}_{k+1} = \mathbf{A}\mathbf{P}_k\mathbf{A}^T + \mathbf{R}, \quad (67)$$

with \mathbf{R} defined in (61). Because the matrix \mathbf{A} is stable the covariance converges to an steady value $\lim_{k \rightarrow \infty} \mathbf{P}_k = \mathbf{P}$ which must satisfy the Lyapunov equation (61).

Combining this \mathbf{P} with (65)-(66) the OCC $\|H\|_2$ constraint becomes

$$\gamma = \sqrt{\frac{\text{tr}(C\mathbf{P}_x C^T) + \text{tr}(R_2)}{\text{tr}(R_2) + \text{tr}(R_1)}} \leq \bar{\gamma}. \quad (68)$$

Rearranging this leads to the condition (62). \blacksquare

Next we present Lemma 5 to compute the optimal value of the OCC $\|H\|_2$ gain and the corresponding optimal controller and observer gain matrices.

Lemma 5 *Given the dynamics in (57), the smallest output covariance constrained $\|H\|_2$ gain defined by (59) is*

$$\gamma^* = \sqrt{\frac{\text{tr}(C\mathbf{P}_x^* C^T) + \text{tr}(R_2)}{\text{tr}(R_2) + \text{tr}(R_1)}}, \quad (69)$$

where $\mathbf{P}_x^* = E_x^T \mathbf{P}^* E_x$ is the state covariance which minimizes (69) and is characterized by the optimal gains L^* , K^* . The solution (L^*, K^*) is found by satisfying the following system of $np + mn$ nonlinear equations,

$$\begin{cases} \text{tr}(C E_x \mathbf{P}_L^{ij} E_x^T C^T) = 0, & i \in \overline{1, n}, j \in \overline{1, p}, \\ \text{tr}(C E_x \mathbf{P}_K^{uv} E_x^T C^T) = 0, & u \in \overline{1, m}, v \in \overline{1, n}. \end{cases} \quad (70)$$

Here \mathbf{P}_L^{ij} and \mathbf{P}_K^{uv} are functions of L and K given in (\star) .

Proof: When the minimum value of γ is reached the inequality (68) changes to equality, which results in (69). We find the stationary points of (69) with respect to each element of L and K ,

$$\nabla \gamma = \left(\frac{\partial \gamma}{\partial L_{ij}} \quad \frac{\partial \gamma}{\partial K_{uv}} \right) = 0, \quad (71)$$

which provides a system of $np + mn$ equations. Since

$$\begin{aligned} \mathbf{P}_L^{ij} &= \sum_{q=0}^{k^*} A^q \begin{bmatrix} 0 & 0 \\ 0 & J_L^{ij} R_2 L^T + L R_2 (J_L^{ij})^T \end{bmatrix} A^{qT} - \sum_{q=1}^{k^*} \left(\sum_{r=1}^q A^{r-1} \begin{bmatrix} 0 & 0 \\ 0 & J_L^{ij} C \end{bmatrix} A^{q-r} R A^{qT} + \sum_{r=1}^q \left(A^{r-1} \begin{bmatrix} 0 & 0 \\ 0 & J_L^{ij} C \end{bmatrix} A^{q-r} R A^{qT} \right)^T \right) \\ \mathbf{P}_K^{uv} &= \sum_{q=1}^{k^*} \left(\sum_{r=1}^q A^{r-1} \begin{bmatrix} G J_K^{uv} & -G J_K^{uv} \\ 0 & 0 \end{bmatrix} A^{q-r} R A^{qT} + \sum_{r=1}^q \left(A^{r-1} \begin{bmatrix} G J_K^{uv} & -G J_K^{uv} \\ 0 & 0 \end{bmatrix} A^{q-r} R A^{qT} \right)^T \right), \quad \begin{matrix} i \in \overline{1, n}, j \in \overline{1, p} \\ u \in \overline{1, m}, v \in \overline{1, n} \end{matrix} \quad (\star) \end{aligned}$$

$\text{tr}(R_1)$ and $\text{tr}(R_2)$ are constants (71) becomes

$$\begin{aligned} \frac{\partial \text{tr}(C E_x \mathbf{P} E_x^T C^T)}{\partial L_{ij}} &= \text{tr} \left(C E_x \frac{\partial \mathbf{P}}{\partial L_{ij}} E_x^T C^T \right) = 0, \\ \frac{\partial \text{tr}(C E_x \mathbf{P} E_x^T C^T)}{\partial K_{uv}} &= \text{tr} \left(C E_x \frac{\partial \mathbf{P}}{\partial K_{uv}} E_x^T C^T \right) = 0, \end{aligned} \quad (72)$$

with $np + mn$ different variables as the components of gain matrices L and K . Thus the system of equations corresponding to optimal γ can be written in the form of (70), where

$$\mathbf{P}_K^{uv} = \frac{\partial \mathbf{P}}{\partial K_{uv}} \quad \text{and} \quad \mathbf{P}_L^{ij} = \frac{\partial \mathbf{P}}{\partial L_{ij}}.$$

Recall the covariance \mathbf{P} is the solution of the Lyapunov equation (61), which can be approximated by the truncated sum

$$\mathbf{P} \approx \sum_{q=0}^{k^*} A^q R A^{qT}, \quad (73)$$

which is a function of the gains L and K . Taking derivatives of (73) with respect to L_{ij} and K_{uv} results in (\star) . \blacksquare

We implement Lemma 5 with the `fsolve` command in MATLAB for (70), using the multi-start option to cast a wide net for the near-global solution. We reject local maximums and saddle points by checking $\nabla^2 \Omega_{k^*} > 0$ (locally for the given answer).

5 Design

In this section we combine the results from the prior two sections to design the optimal gains L and K to minimize the impact of the attack while satisfying a chosen performance criteria. Specifically, the optimal pair (L, K) is designed to minimize the trace of the minimum ellipsoid containing the reachable set while maintaining the OCC $\|H\|_2$ gain less than an assigned threshold $\bar{\gamma}$. For feasibility the OCC $\|H\|_2$ gain $\bar{\gamma}$ should be selected to be no smaller than the smallest possible OCC $\|H\|_2$ gain γ^* , i.e., $\bar{\gamma} \geq \gamma^*$. On the other hand, to avoid the trivial $L = 0$ and/or $K = 0$ solution, this desired OCC $\|H\|_2$ gain should be smaller than the open loop noise-to-output gain, denoted γ_0 , i.e., $\bar{\gamma} < \gamma_0$.

Lemma 6 *Given the system dynamics (54) and (55), the open loop (i.e., $L = 0$ or $K = 0$) OCC $\|H\|_2$ gain γ_0 is given by*

$$\gamma_0 = \sqrt{\frac{\text{tr}(C \mathbf{P}_x C^T) + \text{tr}(R_2)}{\text{tr}(R_2) + \text{tr}(R_1)}}, \quad (74)$$

where the steady state covariance of state \mathbf{P}_x is the solution of

$$F \mathbf{P}_x F^T - \mathbf{P}_x + R_1 = 0. \quad (75)$$

Proof. For both $L = 0$ or $K = 0$, the state dynamics (54) are in open loop and thus the evolution of the system is the same. When $L = 0$, the state estimate \hat{x}_k converges to zero because the system is open loop stable, but the actual state x_k does not due to the influence of noise. Thus the open loop state dynamic becomes

$$x_{k+1} = e_{k+1} = F e_k + \nu_k. \quad (76)$$

Similarly, when $K = 0$, equation (54) directly becomes

$$x_{k+1} = F x_k + \nu_k. \quad (77)$$

With this state equation, the steady state covariance of the state, \mathbf{P}_x , is given by (75) and consequently the performance threshold γ_0 should be the same in both cases. \blacksquare

Together these limits define the possible range of $\bar{\gamma}$ which we call the *trade off interval*,

$$\gamma^* \leq \bar{\gamma} \leq \gamma_0. \quad (78)$$

For systems with highly stable open loop system matrix F , this trade off interval is relatively small because γ_0 is already relatively small. For systems that are close to marginal stability (eigenvalues of F close to the unit circle) the trade off interval is larger. The stability of F is also a major factor in the size of the reachable set, so such marginal systems are more sensitive to both noise and attacks.

Theorem 3 *Given the system matrices F, G, C and performance threshold $\bar{\gamma} \in [\gamma^*, \gamma_0]$, zero mean process*

$$\sum_{q=1}^{k^*} \frac{\text{tr}((H_q^T H_q)(J_L^{ij} \Sigma L^T + L C E_e \mathbf{P}_L^{ij} E_e^T C^T L^T + L \Sigma J_L^{ijT}))}{2\sqrt{\text{tr}(H_q L \Sigma L^T H_q^T)}} = -\lambda \text{tr}(C E_x \mathbf{P}_L^{ij} E_x^T C^T), \quad \begin{matrix} i \in \overline{1, n}, j \in \overline{1, p} \\ E_e = [0_n, I_n] \end{matrix} \quad (\dagger)$$

$$\sum_{q=1}^{k^*} \frac{\sum_{r=1}^q \text{tr}(2L \Sigma L^T H_q^T (F + GK)^{r-1} (G J_K^{uv}) (F + GK)^{q-r})}{2\sqrt{\text{tr}(H_q L \Sigma L^T H_q^T)}} = -\lambda \text{tr}(C E_x \mathbf{P}_K^{uv} E_x^T C^T), \quad u \in \overline{1, m}, v \in \overline{1, n} \quad (\ddagger)$$

and sensor noise with covariances R_1 and R_2 , the solution of (\dagger) , (\ddagger) and

$$\text{tr}(C E_x \mathbf{P} E_x^T C^T) + \text{tr}(R_2) - \bar{\gamma}^2 (\text{tr}(R_1) + \text{tr}(R_2)) = 0, \quad (79)$$

yields optimal gains L^* , K^* that minimize the attack impact while satisfying the OCC $\|H\|_2$ condition.

Proof: The minimum trace ellipsoid that bounds the reachable set is $\mathcal{E}(Q^*)$. We use the trace of the shape matrix as a proxy for the impact of the attack, i.e., we aim to minimize

$$\sqrt{\text{tr}(Q^*)} = \sum_{i=0}^{k^*} \left(\sqrt{\alpha} \sqrt{\text{tr}(H_i L \Sigma L^T H_i^T)} + \sqrt{\bar{\nu} \text{tr}(F^i R_1 F^{iT})} \right), \quad (80)$$

which decomposes the ellipsoidal bound on the reachable set into contributions from the noise and attack.

Remark 2 Because the portion of the impact due to noise in (80) is not a function of gain matrices L and K , it does not play a role in minimizing the attack impact. In addition, the threshold α , which is selected based on the noise distribution and the detector's desired false alarm rate, is also not a function of L and K . Since it appears as a uniform scaling factor it also does not play a role in minimizing the attack impact. These are both distinct advantages for selecting an objective that minimizes the trace of the shape matrix of the ellipsoid bound (as opposed to, e.g., minimizing the volume). This feature is not present in the convexified version of this problem [14].

From Remark 2, we can reduce (80) to the following objective function

$$\mathcal{J}_{k^*} = \sum_{i=0}^{k^*} \sqrt{\text{tr}(H_i L \Sigma L^T H_i^T)}. \quad (81)$$

This separation of noise and attack and the ability to remove the threshold α is a special property that comes from selecting the minimum trace ellipsoid (Lemma 2) and a cost function to minimize the trace of the ellipsoidal bound (other work has used the volume, i.e., $\det(Q^*)$, as the measure to minimize to reduce attack impact, e.g., [16]). A consequence of these facts is that the noise truncation probability \bar{p} also does not appear

in \mathcal{J}_{k^*} . This implies that the optimal observer gain and controller gain can be computed independent from the choice of truncation used to bound the noise.

We motivated a performance constraint, in this case the OCC $\|H\|_2$ constraint, in order to avoid the trivial $L = 0$ or $K = 0$ solutions. It is intuitive, and can be seen in (81), that over the trade off interval $\bar{\gamma} \in [\gamma^*, \gamma_0]$ the objective \mathcal{J}_{k^*} decreases as, e.g., L approaches zero, however, the OCC $\|H\|_2$ gain γ is increasing as it approaches γ_0 . Thus we expect for $\bar{\gamma} \in [\gamma^*, \gamma_0]$ that the optimal L^* and K^* to minimize the attack impact \mathcal{J}_{k^*} will occur at $\gamma = \bar{\gamma}$. We use this observation to change (62) from an inequality to equality $\mathcal{C}_{k^*} = 0$, which simplifies the process of including the OCC $\|H\|_2$ constraint as a Lagrange multiplier in the optimization,

$$\Omega_{k^*} = \mathcal{J}_{k^*} + \lambda \mathcal{C}_{k^*}, \quad \gamma^* \leq \bar{\gamma} \leq \gamma_0. \quad (82)$$

The necessary condition for a local minimum indicates that the optimum values of K , L and scalar λ satisfy

$$\nabla \Omega_{k^*} = \left(\frac{\partial \Omega_{k^*}}{\partial L_{ij}} \quad \frac{\partial \Omega_{k^*}}{\partial K_{uv}} \quad \frac{\partial \Omega_{k^*}}{\partial \lambda} \right) = 0, \quad (83)$$

where the equations in (\dagger) , (\ddagger) , and (79) correspond to each term of the gradient being zero, respectively.

Finally, note that the stabilizability and detectability of the system along with the output covariance being bounded (ensured by the $\|H\|_2$ constraint) guarantees the state covariance to be bounded - hence the optimal L and K found through this theorem ensure a stable closed loop system. ■

As before we use `fsolve` with (\dagger) , (\ddagger) , and (79) (with multi-start option) and numerically ensure the solution is a minimum.

By increasing the value of $\bar{\gamma}$, the optimum value of $\text{tr}(Q^*)$ decreases, which implies a trade-off between the system performance (OCC $\|H\|_2$ gain) and security (size of the reachable set). Recall that for $\bar{\gamma} \geq \gamma_0$ then $L = 0$ or $K = 0$ and the attack has no impact. Note then that the entire reachable set is determined only by the contribution due to the noise (the attack portion is zero)

$$\sqrt{\text{tr}(Q^*)} = \sum_{i=0}^{k^*} \sqrt{\bar{\nu} \text{tr}(F^i R_1 F^{iT})}. \quad (84)$$

6 Case Study

We now demonstrate these tools and provide the trade off curve between system performance and security as the performance constraint is varied. We consider an LTI system with matrices,

$$F = \begin{bmatrix} 1.04 & -0.14 \\ 0.30 & 0.63 \end{bmatrix}, G = \begin{bmatrix} 2 & 3 \\ 1 & 1 \end{bmatrix}, C = \begin{bmatrix} 2 & 2 \\ 1 & 2 \end{bmatrix}, \quad (85)$$

$$R_1 = \begin{bmatrix} 0.018 & -0.022 \\ -0.022 & 0.026 \end{bmatrix}, R_2 = \begin{bmatrix} 0.0018 & 0.0031 \\ 0.0031 & 0.0096 \end{bmatrix},$$

equipped with a chi-squared detector tuned to a false alarm rate of 5% ($\alpha = 5.99$), and with process noise truncated at $\bar{p} = 95\%$ ($\bar{p} = 5.99$). We select a settling time of $k^* = 35$.

Using Lemma 5, we identify the minimum OCC $\|H\|_2$ gain $\gamma^* = 1.57$, which is achieved by

$$L = \begin{bmatrix} 1.00 & -0.97 \\ -0.01 & 0.26 \end{bmatrix}, \quad K = \begin{bmatrix} 0.14 & -2.04 \\ -0.44 & 1.41 \end{bmatrix}. \quad (86)$$

Using (80) we can then calculate the security metric based on the set of states reachable by a stealthy zero-alarm attacker, $\sqrt{\text{tr}(Q^*)} = 16.82^1$. Of the observer and controller gain matrices that achieve γ^* , here we have selected the pair with the smallest value of $\sqrt{\text{tr}(Q^*)}$. This point is plotted in Figure 4 with a red asterisk (*).

From Lemma 6, the open loop OCC $\|H\|_2$ gain $\gamma_0 = 10.18$.

We now solve Theorem 3 over the trade off interval $\bar{\gamma} \in [\gamma^*, \gamma_0]$ to identify the observer and controller gains that minimize the attacker's impact while still satisfying the OCC $\|H\|_2$ gain constraint $\bar{\gamma}$. In Figure 4, these minimum reachable sets define a curve (black) that quantifies the fundamental trade off between performance and security - that demanding improved performance (smaller γ) necessarily increases the impact an attacker can have on the system (even if the operator is using the best choice of observer and controller gains). The optimization landscape yields a more difficult problem to solve as $\bar{\gamma}$ approaches γ^* ; we were able to find solutions down to $\bar{\gamma} = 1.59$.

In companion work, we have explored this same idea through the use of convex optimization and linear matrix inequalities, replacing the geometric approach here

¹ Using the convex optimization presented in Theorem 1 of [14], we can confirm that this is indeed the global minimum OCC $\|H\|_2$ gain and the corresponding L and K (with smallest reachable set).

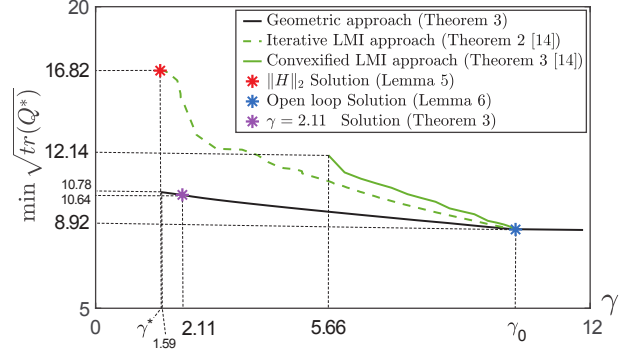


Figure 4. Performance-security curve for the proposed nonlinear Geometric approach (black) compared with two semi-definite optimization approaches (green), one of which uses an iterative scheme to eliminate some nonlinearities and one is fully linearized. The extra steps taken to linearize the problem make the fully convex optimization feasible only for a portion of the entire trade off interval.

with a Lyapunov-type method to provide an ellipsoidal bound on the reachable set [14]. The advantage of a convex optimization approach is the existence of a unique global optimum and fast computation times, however, such clean solutions typically require approximations that add additional conservatism to the results. In this paper we formulate a nonlinear optimization which may have a complex optimization landscape with multiple local minima, however, it does not include any extra margins of conservatism in the solution. In Figure 4 we compare the current paper's geometric approach (black) with two convex optimization approaches developed in [14] (green and dashed green). The proposed nonlinear optimization finds observer and controller gains that constrain attackers to smaller reachable sets than the LMI approaches. This security advantage is particularly noticeable at near-optimal performance values (γ close to γ^*). The geometric approach helps to identify the fundamental trade off between security and performance, highlighting, for example, the fact that giving up a small amount of performance can lead to a dramatic improvement in security (changing $\bar{\gamma}$ from γ^* to $\gamma^* + \epsilon$). This is less obvious from the convex optimization approaches.

In Figure 5 we compare the ellipsoidal bounds on reachable sets between the OCC $\|H\|_2$ optimal L and K - i.e., when $\bar{\gamma} = \gamma^*$, and two other points on the trade off curve $\bar{\gamma} = \gamma_0$ (open loop) and $\bar{\gamma} = 2.11$. At $\bar{\gamma} = \gamma_0$, $L = 0$ and/or $K = 0$ and the attack impact is at its minimum. In Figure 5a we plot the entire reachable set bounding ellipsoid, (80), (noise and attack) and in Figure 5b we plot the part due only to the attack (81). As discussed, in open loop the attack contribution is zero (see blue dot with zero volume in Fig 5b). The entire reachable set is nonzero due to the noise contributions, which is why in Figure 4, $\sqrt{\text{tr}(Q^*)} = 8.92$ - see (84).

Figure 5 also demonstrates how a relatively small in-

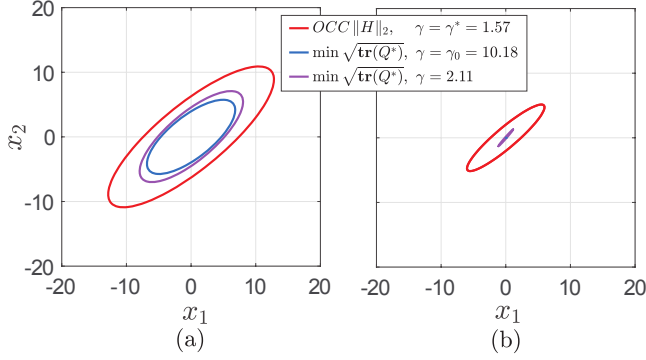


Figure 5. Comparison of the ellipsoidal outer bound of the reachable set for $\bar{\gamma} = \gamma^*$ (red), $\bar{\gamma} = 2.105$ (purple), and $\bar{\gamma} = \gamma_0$ (blue) due to (a) noise and attack contributions and (b) only attack contribution. As expected, in open loop the attack impact is zero.

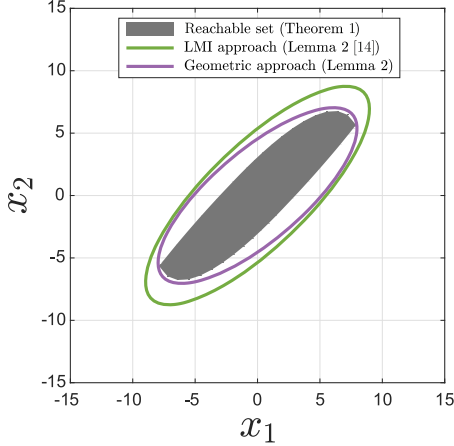


Figure 6. For the observer and controller gains in (87) corresponding to $\bar{\gamma} = 2.11$, the geometric approach leads to a tighter ellipsoidal bound on the true reachable set, when compared with the LMI approach used in [14].

crease in $\bar{\gamma}$ (from $\gamma^* = 1.57$, to $\gamma = 2.11$), corresponding to a decrease in performance, is able to reduce the reachable set of the system under attack (from the red ellipsoid to the purple ellipsoid, respectively). For $\bar{\gamma} = 2.11$, the gain matrices L and K are

$$L = \begin{bmatrix} 0.24 & -0.21 \\ 0.46 & -0.40 \end{bmatrix}, \quad K = \begin{bmatrix} -1.34 & -1.70 \\ 0.69 & 0.87 \end{bmatrix}. \quad (87)$$

For this choice of L and K , in Figure 6 we show a comparison of the tightness of the ellipsoidal bounds provided by the geometric and LMI tools. The exact reachable set (gray) is computed using Theorem 1. The geometric approach (purple ellipse) fits an outer ellipsoidal bound using Lemma 2. The LMI approach (green) uses the analysis result, Lemma 2, from [14] to find an outer ellipsoidal bound using a Lyapunov-type method. We observe that the geometric approach yields a tighter outer bound.

Conclusion

Reachable set computations based on geometric sums have been explored and developed in the past, e.g., [17]. The new geometric results we present here enable us to create the optimization to tune to co-design of performance, measured by an output covariance constrained $\|H\|_2$ gain, and security, measured by the size of the ellipsoidal bound on the reachable set of attacked states. The ellipsoidal tools we develop facilitate an elegant separation - by using the minimum trace ellipsoid - between contributions based on noise and based on attacks.

We find that by giving up a small amount of closed-loop performance, we can significantly reduce the vulnerability of the system to attack. The geometric approach is able to recover consistent optimization solutions along the trade-off interval between optimal $\|H\|_2$ closed-loop and open-loop performance. While the alternative approach provides linear matrix inequalities to be solved, the relaxations required to convexify the problem ultimately yield poorer solutions, especially as the performance criteria is pushed closer to optimal.

At a higher level, our geometric tools provide the exact boundary of the geometric sum of a number of ellipsoids and ensure tight ellipsoidal bounds on the exact geometric sum. We believe these results will be valuable for broader work with geometric sums and reachable sets outside the realm of security.

References

- [1] C. G. Rieger, D. I. Gertman, and M. A. McQueen, "Resilient control systems: Next generation design research," in *2009 2nd Conference on Human System Interactions*. IEEE, 2009, pp. 632–636.
- [2] L. Mili and N. V. Center, "Taxonomy of the characteristics of power system operating states," in *2nd NSF-VT Resilient and Sustainable Critical Infrastructures (RESIN) Workshop*, 2011, pp. 13–15.
- [3] L. Mili and S. Shukla, "Power and communications systems as integrated cyberphysical systems," in *Proc. of 48th Allerton Conference on Communication, Control, and Computing, Allerton, IL*, 2010.
- [4] Y. Shoukry, M. Chong, M. Wakaiki, P. Nuzzo, A. Sangiovanni-Vincentelli, S. A. Seshia, J. P. Hespanha, and P. Tabuada, "Smt-based observer design for cyber-physical systems under sensor attacks," *ACM Transactions on Cyber-Physical Systems*, vol. 2, no. 1, pp. 1–27, 2018.
- [5] H. Fawzi, P. Tabuada, and S. Diggavi, "Secure estimation and control for cyber-physical systems under adversarial attacks," *IEEE Transactions on Automatic control*, vol. 59, no. 6, pp. 1454–1467, 2014.
- [6] K. Saulnier, D. Saldana, A. Prorok, G. J. Pappas, and V. Kumar, "Resilient flocking for mobile robot teams," *IEEE Robotics and Automation letters*, vol. 2, no. 2, pp. 1039–1046, 2017.

- [7] H. J. LeBlanc, H. Zhang, X. Koutsoukos, and S. Sundaram, "Resilient asymptotic consensus in robust networks," *IEEE Journal on Selected Areas in Communications*, vol. 31, no. 4, pp. 766–781, 2013.
- [8] M. Zhu and S. Martinez, "On the performance analysis of resilient networked control systems under replay attacks," *IEEE Transactions on Automatic Control*, vol. 59, no. 3, pp. 804–808, 2013.
- [9] K. Zhou and J. C. Doyle, *Essentials of robust control*. Prentice hall Upper Saddle River, NJ, 1998, vol. 104.
- [10] T. Başar and P. Bernhard, *H-infinity optimal control and related minimax design problems: a dynamic game approach*. Springer Science & Business Media, 2008.
- [11] Y. Mo and B. Sinopoli, "On the performance degradation of cyber-physical systems under stealthy integrity attacks," *IEEE Transactions on Automatic Control*, vol. 61, pp. 2618–2624, 2016.
- [12] C. Murguia and J. Ruths, "On reachable sets of hidden cps sensor attacks," in *American Control Conference*, 2018.
- [13] C. Murguia, I. Shames, J. Ruths, and D. Nešić, "Security metrics and synthesis of secure control systems," *Automatica*, vol. 115, p. 108757, 2020.
- [14] N. Hashemi and J. Ruths, "Co-design for performance and security: Lmi tools," *Automatica*, Submitted. [Online]. Available: arXiv:1909.12452
- [15] S. H. Kafash, J. Giraldo, C. Murguia, A. A. Cardenas, and J. Ruths, "Constraining attacker capabilities through actuator saturation," in *2018 Annual American Control Conference (ACC)*. IEEE, 2018, pp. 986–991.
- [16] N. Hashemi, C. Murguia, and J. Ruths, "A comparison of stealthy sensor attacks on control systems," in *2018 Annual American Control Conference (ACC)*. IEEE, 2018, pp. 973–979.
- [17] A. A. Kurzhanskiy and Varaiya, *Ellipsoidal calculus for estimation and control*. Nelson Thornes, 1997.
- [18] C. Murguia and J. Ruths, "On model-based detectors for linear time-invariant stochastic systems under sensor attacks," *IET Control Theory & Applications*, vol. 13, no. 8, pp. 1051–1061, 2019.
- [19] D. Umsonst and H. Sandberg, "Anomaly detector metrics for sensor data attacks in control systems," in *2018 Annual American Control Conference (ACC)*. IEEE, 2018, pp. 153–158.
- [20] A. A. Kurzhanskiy and P. Varaiya, "Ellipsoidal toolbox (et)," in *Decision and Control, 2006 45th IEEE Conference on*. IEEE, 2006, pp. 1498–1503.
- [21] G. Zhu, M. Rotea, and R. Skelton, "A convergent algorithm for the output covariance constraint control problem," *SIAM Journal on Control and Optimization*, vol. 35, no. 1, pp. 341–361, 1997.

A Novelty of the Minimum Trace Bound

Lemma 2 identified the *unique* p_{ij} parameters that yield the minimum trace shape matrix for the outer bound of the geometric sum, $p_{ij}^* = \sqrt{\text{tr}(Q_j)/\text{tr}(Q_i)}$. For (50) to be true, there would need to exist an $\ell \in \mathbb{R}^n$ such that

$$p_{ij} = \frac{\langle \ell, Q_j \ell \rangle^{\frac{1}{2}}}{\langle \ell, Q_i \ell \rangle^{\frac{1}{2}}} = \sqrt{\frac{\text{tr}(Q_j)}{\text{tr}(Q_i)}}, \quad \forall (i, j) \in \mathcal{I}. \quad (\text{A.1})$$

Since ℓ has n elements and is restricted to have unit length ($\|\ell\| = 1$), there are $n - 1$ unknowns in (A.1). For the shape matrices Q_1, \dots, Q_k , the index set \mathcal{I} has $\binom{k}{2}$ elements, and by assumption $d > n$ of the k shape matrices are linearly independent. What we will show is that $d > n$ linearly independent shape matrices leads to more equations (constraints) than can be satisfied through the $n - 1$ unknowns in ℓ .

To see this, without loss of generality, assume the numbering is such that the first d shape matrices are linearly independent and define the corresponding index set $\mathcal{I}_d = \{(i, j) \mid 1 \leq i < j \leq d, i, j \in \mathbb{N}\} \subseteq \mathcal{I}$. The linear independence means that

$$\sum_{i=1}^d \alpha_i Q_i = 0_{n \times n} \quad \Rightarrow \quad \alpha_i = 0 \quad \forall i \in \overline{1, d}, \quad (\text{A.2})$$

i.e., the sum being zero implies that all the coefficients must be zero. Now we specifically consider the index set $\mathcal{I}_1 = \{(1, j) \mid 1 < j \leq d, j \in \mathbb{N}\} \subseteq \mathcal{I}_d$. Over this index set, (A.1) enumerates $d - 1$ equations,

$$\frac{\langle \ell, Q_1 \ell \rangle}{\text{tr}(Q_1)} = \frac{\langle \ell, Q_j \ell \rangle}{\text{tr}(Q_j)}, \quad j \in \overline{2, d}. \quad (\text{A.3})$$

We claim all the equations provided by (A.3) are independent. To justify this, we show that the functions that define these equations, i.e.,

$$f_j(\ell) = \ell^T \left(Q_1 - \frac{\text{tr}(Q_1)}{\text{tr}(Q_j)} Q_j \right) \ell, \quad (\text{A.4})$$

for $j \in \overline{2, d}$ are linearly independent, where (A.3) becomes $f_j(\ell) = 0$. These functions are linearly independent if

$$\sum_{j=2}^d \beta_j f_j(\ell) = 0 \quad \Rightarrow \quad \beta_j = 0 \quad \forall j \in \overline{2, d}. \quad (\text{A.5})$$

Note that the functions being linearly dependent requires the sum to be identically zero over all choices of ℓ . Thus, expanding,

$$\sum_{j=2}^d \beta_j \ell^T \left(Q_1 - \frac{\text{tr}(Q_1)}{\text{tr}(Q_j)} Q_j \right) \ell = 0, \quad (\text{A.6})$$

would imply the coefficients must be zero if the functions are linearly independent. Since this relation must hold for all choices of ℓ , we can remove the inner product

$$\sum_{j=2}^d \beta_j \left(Q_1 - \frac{\text{tr}(Q_1)}{\text{tr}(Q_j)} Q_j \right) = \sum_{j=1}^d \alpha_j Q_j = 0_{n \times n}, \quad (\text{A.7})$$

with $\alpha_1 = \sum_{j=2}^d \beta_j$ and $\alpha_j = -\beta_j \frac{\text{tr}(Q_1)}{\text{tr}(Q_j)}$ for $j \in \overline{2, d}$. However, this contradicts the assumption that matrices Q_1, \dots, Q_d are linearly independent (A.2). This implies that the functions $f_j(\ell)$ are linearly independent, which show that the $d-1$ equations in (A.3) are independent and cannot be satisfied by the $n-1$ unknowns in ℓ since $n-1 < d-1$.

So far we have only considered $(i, j) \in \mathcal{I}_1$. For the remaining choices $(i, j) \in \mathcal{I}_d \setminus \mathcal{I}_1$, we show that they produce equations that are redundant to those in \mathcal{I}_1 . For some $(i, j) \in \mathcal{I}_d$ (A.1) is effectively the same as combining two equations from \mathcal{I}_1 ,

$$\frac{\langle \ell, Q_i \ell \rangle}{\text{tr}(Q_i)} = \frac{\langle \ell, Q_j \ell \rangle}{\text{tr}(Q_j)} \Leftrightarrow \begin{cases} \frac{\langle \ell, Q_1 \ell \rangle}{\text{tr}(Q_1)} = \frac{\langle \ell, Q_i \ell \rangle}{\text{tr}(Q_i)} \\ \frac{\langle \ell, Q_1 \ell \rangle}{\text{tr}(Q_1)} = \frac{\langle \ell, Q_j \ell \rangle}{\text{tr}(Q_j)} \end{cases} \quad (\text{A.8})$$

This demonstrates that there are $d-1$ independent equations generated by considering (A.1) over the index set \mathcal{I}_d .

Finally we show that including the remaining indices in the original set \mathcal{I} does not introduce any additional independent equations. By assumption of their linear dependence, the remaining shape matrices Q_i and Q_j , $(i, j) \in \mathcal{I} \setminus \mathcal{I}_d$, can be written as $Q_i = \sum_{r=1}^d a_r Q_r$ and $Q_j = \sum_{r=1}^d b_r Q_r$. The relationship between the first d matrices was established in (A.3) as

$$\frac{\langle \ell, Q_1 \ell \rangle}{\text{tr}(Q_1)} = \frac{\langle \ell, Q_2 \ell \rangle}{\text{tr}(Q_2)} = \dots = \frac{\langle \ell, Q_d \ell \rangle}{\text{tr}(Q_d)}. \quad (\text{A.9})$$

Multiplying numerator and denominator by arbitrary scalars a_r and b_r , $r \in \overline{1, d}$, does not change this equality,

$$\begin{aligned} \frac{a_1 \langle \ell, Q_1 \ell \rangle}{a_1 \text{tr}(Q_1)} &= \dots = \frac{a_d \langle \ell, Q_d \ell \rangle}{a_d \text{tr}(Q_d)} \\ &= \frac{b_1 \langle \ell, Q_1 \ell \rangle}{b_1 \text{tr}(Q_1)} = \dots = \frac{b_d \langle \ell, Q_d \ell \rangle}{b_d \text{tr}(Q_d)}. \end{aligned} \quad (\text{A.10})$$

Now recall the simple fractional relation that if $a/b = c/d$, then $(a+c)/(b+d)$. Using this, we combine the equations above to show

$$\frac{\sum_{r=1}^d a_r \langle \ell, Q_r \ell \rangle}{\sum_{r=1}^d a_r \text{tr}(Q_r)} = \frac{\sum_{r=1}^d b_r \langle \ell, Q_r \ell \rangle}{\sum_{r=1}^d b_r \text{tr}(Q_r)} \quad (\text{A.11})$$

$$\frac{\langle \ell, Q_i \ell \rangle}{\text{tr}(Q_i)} = \frac{\langle \ell, Q_j \ell \rangle}{\text{tr}(Q_j)} \quad (\text{A.12})$$

Thus, the remaining equations given by $(i, j) \in \mathcal{I} \setminus \mathcal{I}_d$ are redundant.

We have now shown that to use (50) to specify the shape matrix of the minimum trace ellipsoid, it would require

satisfying $d-1$ independent equations with $n-1$ variables (in ℓ). When $d > n$ this is not possible and no ℓ direction can produce the p_{ij} coefficients using (51), thus the family of matrices given by (50) cannot express the minimum trace shape matrix Q^* . ■

B Boundedness of minimum trace ellipsoidal bound

Lemma 7 *If the open-loop state matrix (F) and closed-loop state matrix ($F + GK$) are stable, and input noise ν_k and attack input δ_k are bounded, then the minimum trace ellipsoidal bound $\mathcal{E}(Q^*)$, is bounded.*

Proof: In order to prove this fact first we take a trace of Q^* as it is introduced in (53).

$$\begin{aligned} \text{tr}(Q^*) &= \\ &= \left(\sum_{i=0}^{\infty} \sqrt{\alpha \text{tr}(H_i L \Sigma L^T H_i^T)} + \sqrt{\bar{\nu} \text{tr}(F^i R_1 F^{iT})} \right)^2 \end{aligned} \quad (\text{B.1})$$

therefore,

$$\begin{aligned} \sqrt{\text{tr}(Q^*)} &= \\ &= \sum_{i=0}^{\infty} \sqrt{\alpha \text{tr}(H_i L \Sigma L^T H_i^T)} + \sqrt{\bar{\nu} \text{tr}(F^i R_1 F^{iT})} \end{aligned} \quad (\text{B.2})$$

In (B.2) the terms that are inside the series approaches to zero as i approaches to ∞ , and according to ratio test.

$$\lim_{i \rightarrow \infty} \frac{\sqrt{\alpha \text{tr}(H_{i+1} L \Sigma L^T H_{i+1}^T)}}{\sqrt{\alpha \text{tr}(H_i L \Sigma L^T H_i^T)}} = \max(\|\lambda_{F+GK}\|, \|\lambda_F\|) < 1$$

$$\lim_{i \rightarrow \infty} \frac{\sqrt{\bar{\nu} \text{tr}(F^{i+1} R_1 F^{(i+1)T})}}{\sqrt{\bar{\nu} \text{tr}(F^i R_1 F^{iT})}} = \max(\|\lambda_F\|) < 1$$

(B.3)

where λ , denotes the eigenvalue. This ratio test shows $\text{tr}(Q^*)$ is bounded which means all of the eigenvalues of Q^* (diameters of $\mathcal{E}(Q^*)$) are bounded, which means $\mathcal{E}(Q^*)$ is bounded. ■

C Trivially Minimizing Attack Impact

From (53) but more readily apparent from (23) and (24) it can be seen that selecting $L = 0$ or $K = 0$ is an attractive choice for minimizing the reachable set due to attack inputs. More specifically regarding the presence of random variable δ_k , (24) suggests that L could be chosen such that $H_i L \Sigma^{\frac{1}{2}} = 0$, $i = 1, 2, \dots, k^*$, but since

Σ is full rank (as a covariance matrix), $H_i L = 0$ which results to,

$$\begin{aligned}
GKL &= 0, & i &= 1 \\
GKFL &= 0, & i &= 2 \\
GKF^2L &= 0, & i &= 3 \\
&\vdots \\
GKF^{n-1}L &= 0, & i &= n.
\end{aligned} \tag{C.1}$$

This implies $GKF^{i-1}L = 0$, therefore, if there exists a common null space for all matrices GKF^i then there are nonzero L matrices that would yield zero attack impact. For example, if matrices GK and F have common null space. Similarly (24) suggests that $GK = 0$, however if G is a full rank matrix, $K = 0$. However, $L = 0$ and/or $K = 0$ are the only generic choices that yield zero attack impact without system-specific information.